DESIGNS OF CREEP RUPTURE CRITERION AND DAMAGE EQUATION FOR LOW Cr ALLOY T/P22 STEEL

Dezheng LIU[1], Zhongren WANG[2], Tao QIN[3], Qihua XU[4]

Creep rupture criterion and damage equation are important in numerical investigation of high temperature creep of structural components. Various microstructures can be developed in low Cr alloy; T/P22 steel, which can enable different combinations of properties for various extreme environments in advanced nuclear systems. In this paper, the mechanisms for microstructural deformation and the evolution of creep cavity on thermal creep of low Cr alloys are investigated. The creep rupture criterion and damage equation to depict the evolution of damage and stress exponents based on tensile creep data of low Cr alloy T/P22 steel are proposed. The accuracy of the proposed damage equation and criterion is demonstrated and verified. Important novelties involved with this criterion and damage equation are determination of unknowns such as low stress, transitional stress and high stress levels on creep damage analytically.

Keywords: Creep; Rupture Criterion; Constitutive Damage Equation; T/P22 Steel; Coalescence.

1. Introduction

Demands on the thermal efficiency lead to an increase in operating temperature of structural components and such structural components experience more creep deformation and damage leading to rupture [1]. Low Cr alloys are mostly utilized in structural components such as steam pipes, turbine generators and reactor pumps operating at high temperatures from 400℃ to 700℃ in nuclear power plants [2, 3, 4]. For safe operation, it is necessary at the design stage to predict and understand the creep damage behavior of low Cr alloys under long-term service conditions.

With the development of various remnant lifetime techniques and predictive models of creep behaviour [5, 6, 7, 8], Dyson and Osgerby [9] proposed a typical set of physical creep damage equations for creep deformation

[1] Department of Mechanical Engineering, Hubei University of Arts and Science, Xiangyang, China; Email: liudezheng126@126.com
[2] Department of Mechanical Engineering, Hubei University of Arts and Science, Xiangyang China; Email: hbwlxy_vision@126.com
[3] Department of Mechanical Engineering, Hubei University of Arts and Science, Xiangyang, China; Email: heu_qt@163.com
[4] Wuhan National Laboratory for Optoelectronics, Huazhong Institute of Electro-Optics, Wuhan China; Email: xu.qihua@yahoo.co.uk

in particle-hardened alloys. The Dyson's creep damage constitutive equations are shown as follows:

$$\dot{\varepsilon} = \dot{\varepsilon}_0 \sinh\left[\frac{\sigma(1-H)}{\sigma_0(1-\emptyset)(1-\omega)}\right] \tag{1}$$

$$\dot{H} = \left(\frac{h\dot{\varepsilon}}{3}\right)\left[1-\left(\frac{H}{H^*}\right)\right] \tag{2}$$

$$\dot{\emptyset} = \left(\frac{K_P}{3}\right)(1-\emptyset)^4 \tag{3}$$

$$\dot{\omega} = N\left(\frac{K_N}{\varepsilon_{fu}}\right)\dot{\varepsilon} \tag{4}$$

Where $N = 1$ when $\sigma_1 > 0$ and $N = 0$ when $\sigma_1 \leq 0$. The parameters of $\dot{\varepsilon}_0$, σ_0, h, K_P are material constant and the details of these parameter calculations can be found in [9]. The parameter of K_N has a maximum value of $1/3$, where ε_{fu} is the uniaxial strain at failure. Variable ε represents the creep strain and variable σ represents the applied stress. Variable H is the strain hardening which can take on values ranging from zero to a microstructure-dependent maximum of H^* (<1). Variable $\emptyset$ increases from its initial value of zero towards a theoretical upper limit of unity (never achievable in practice); therefore, decreasing the magnitude of σ_0 will increase creep rate. Variable ω represents the damage induced by continuous cavity nucleation [10].

Dyson's equations have been widely used in the creep damage analysis of high temperature structures, e.g. [10, 11, 12] among other publications. Some deficiencies still exist and can be summarised as: 1) the rupture criterion follows conventional creep damage mechanics and the material is deemed to fail when the creep damage reaches a constant value; however, the damage at failure time may not be a constant in physical practice [13]; 2) the stress breakdown phenomenon has not been involved in this equation as a result of lack of consideration of the effects of changing fracture mechanisms on microstructural changes under different stress levels [14]; 3) predictions overestimate lifetimes at a temperature of 530℃, particularly at low stress level, due to lack of consideration of the cavitation on strain trajectories [9].

The dominant creep deformation and rupture mechanisms are different influenced by the applied stress [15, 16]; and the extrapolation of the use of typical damage equations and stress functions from high stress level to low stress is still under the risk of over-estimating the creep lifetime [17, 18]. Thus, it is important to develop a new creep rupture criterion covers a wide range of the stress suitable for the actual applications of the components.

This paper reports the design of a new creep rupture criterion and damage equation to estimate the evolution of damage and failure times based on tensile creep data for low Cr alloy T/P22 steel under a wide range of stress. It firstly investigates the cavity nucleation and growth through the experimental observation of the evolution of creep cavity in 2.25Cr-1Mo steel. Furthermore, it reports the design creep rupture criterion and damage equation and the determination of unknowns such as low stress, transitional stress and high stress levels on creep damage analytically. Lastly, it demonstrates the validity of the new rupture criterion and damage equation through comparison of simulated results with physically-based creep experiment data.

This work contributes to computational creep damage mechanics in general and particularly to the design and development of a constitutive model for creep damage analysis of low Cr alloys T/P22 steel under long-term service. The accuracy of the proposed damage equation and rupture criterion is demonstrated, and it shows better than the available equations.

2. Research Method

Creep fracture is caused by the processes of nucleation and growth of cavities. With the continued growth of voids, creep cracks grow from the cusp and ultimately weaken the cross section to the point where failure occurs [10]. To understand the physics in a creep damage equation, and then to correct its undesirable features, it is essential to investigate the creep mechanisms which lead to creep rupture; it is also vital to understand the physically-based experiment data involving the minimum creep rate under different stress levels and damage behavior at the different creep stages. The following steps are taken for constructing the creep rupture criterion and damage equation for low Cr alloy T/P22 steel.

1) To investigate the evolution of creep cavity during the rupture process. The characteristics of initial creep cavity and cavity at rupture time should be analyzed, and then the dominative mechanisms during the creep rupture process should be determined. This work was conducted through the observation of the micro-structural changes of 1Cr-0.5Mo steel under the stress 35MPa at temperature of 520℃;

2) To design the creep rupture criterion and damage equation for low Cr alloy T/P22 steel. The material parameter of cavity area fraction equation according to the experimental data on creep rupture time under different stress levels and temperature should be investigated in order to achieve the specific quantitative equation for cavity area fraction along grain boundary based on the appropriate cavity nucleation and cavity growth models, and then a new damage equation based on Dyson's equation [13] should be developed according to the the findings

described in the step 1 and step 2 of the above. Experiment data for the evolution of creep cavity for 2.25Cr-1Mo steel under stresses of 55.6MPa, 60.6MPa and 70.6MPa at a temperature of 565℃ were studied for this work;,

3) To validate the new damage equation and creep rupture criterion. The validation should be conducted through comparison of simulated results with physically-based creep experiment data and conventional Dyson's damage evolution equation [10]. Experiment data for the evolution of creep damage under the stress 40MPa ($0.31\sigma_Y$) (σ_Y is the yield stress) at 640℃ for 0.5Cr0.5Mo0.25V base material are utilized to demonstrate the validity for this work.

3. Results and Discussion

Experimental observation of the evolution of creep cavity

The characteristics of initial creep cavities can be analysed based on the observation of the micro-structural changes of 1Cr-0.5Mo steel under the stress 35MPa at temperature of 520℃. The micro-structure of creep cavities at initial damage time is shown in Fig. 1.

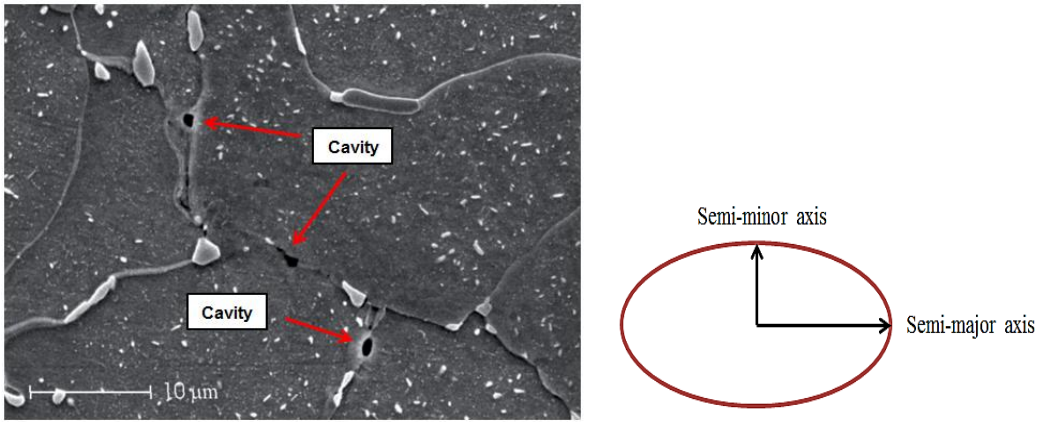

(a) Initial cavities (b) cavity schematic diagram

Fig. 1: Initial cavities of 1Cr-0.5Mo steel under the stress 35MPa at temperature of 520℃ (a) and cavity semi-axis schematic diagram (b)

Fig. 1 displays the cavity at initial damage stage; three cavities have been captured through the use of Scanning Electron Microscopy (SEM). The size and shape of cavities can be represented by a cavity semi-axis schematic diagram. According to the experiment data for cavities at initial damage stage of 1Cr-0.5Mo steel, the radii of initial cavities in the semi-minor axis and semi-major axis can be summarised and plotted as shown in Fig.2.

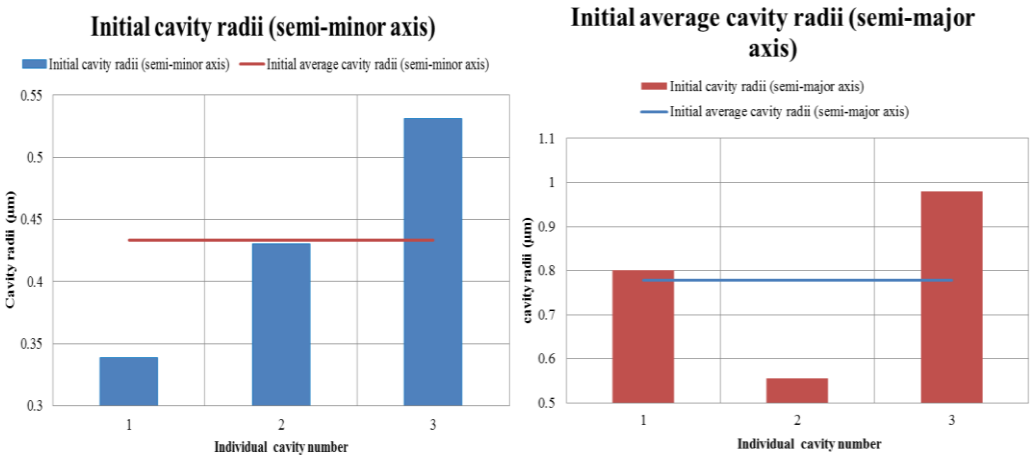

(a) Cavity radii (μm) (b) Cavity radii (μm)

Fig.2: Radii of initial cavities of 1Cr-0.5Mo steel in semi-minor axis (a) and in semi-major axis (b)

Fig.2 displays the radii of initial cavities of 1Cr-0.5Mo steel in semi-minor axis (a) and in semi-major axis (b), respectively. The average initial cavity radius R_i (μm) can be plotted and the value of the average initial cavity radius in semi-minor axis (a) is 0.433 and in the semi-major axis (b). is 0.778.

The characteristics of creep cavity at coalescence stage can be analysed based on the observation of micro-structural changes of 1Cr-0.5Mo steel under the stress 35MPa at temperature of 520℃. The micro-structure of creep cavities at rupture time is shown in Fig. 3.

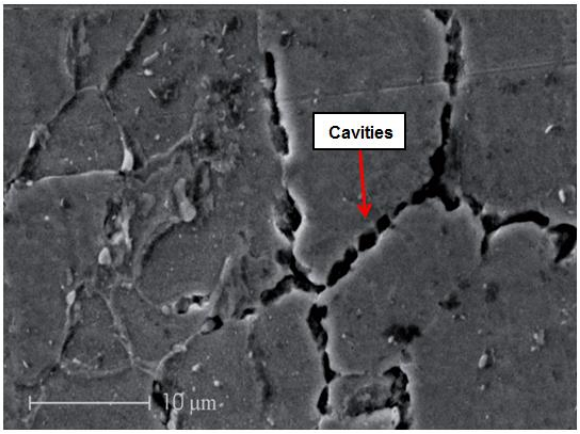

Fig.3: Cavities at coalescence stage of 1Cr-0.5Mo steel under stress range from 35MPa at temperature of 520℃

According to Fig.3, the number of cavities has significantly increased and the characteristics of creep cavities on the fracture surface have been captured through the use of Scanning Electron Microscope (SEM). Cavities coalesce by mid-way through the tertiary stage, though many retain their individuality even at

rupture. Once the size of voids grows sufficiently large, they will coalesce either with nearby cracks or with neighbouring voids. The radii of cavities at coalescence stage in the semi-minor axis (a) and in the semi-major axis (b) can be summarised and plotted as shown in Fig.4.

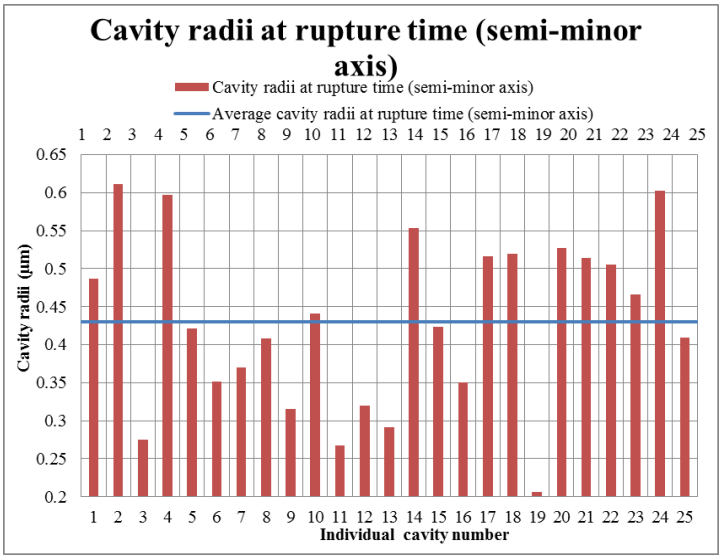

(a) Cavity radii (μm)

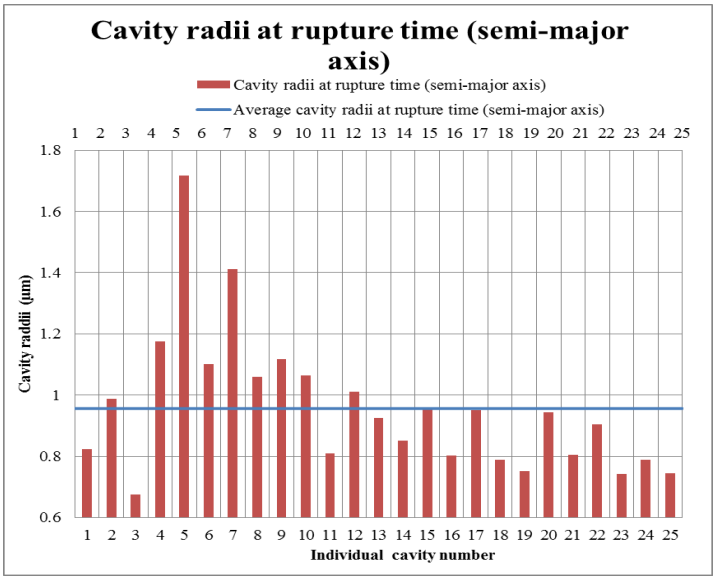

(b) Cavity radii (μm)

Fig.4: Radii of cavities of 1Cr-0.5Mo steel at coalescence stage in the semi-minor axis (a) and in semi-major axis (b)

Fig.4 shows the radii of cavities of 1Cr-0.5Mo steel at coalescence stage in the semi-minor axis (a) and in semi-major axis (b), respectively. The average

cavity radius R_c (μm) at coalescence stage can be plotted and the value of the average cavity radius in semi-minor axis (a) is 0.430 and in semi-major axis (b) is 0.956. The number of cavities has increased from 3 (initial damage stage) to 25 (coalescence stage). Creep rupture is caused by the accumulation of cavity nucleation and growth. At a low stress level, it is usually associated with brittle rupture behaviour and the dominative rupture mechanism is based on cavity nucleation [19]. At high stresses, however, it is normally associated with ductile rupture behaviour and the dominative rupture mechanism is based on cavity growth [19, 20]. Furthermore, the model of cavity growth is controlled by the diffusion process, because the cavity growth process involves vacancy condensation [2].

Dobrzański [21] reported that the majority of cavities appear along the Grain boundary (GB) which is transverse to the stress axis, and that cavity growth is affected by the absorption of excess stress-induced vacancies [21]. Due to the fact that the short radii of cavities are controlled by the GB, the cavity profile can evolve over time into an elongated crack. The evolution of creep cavities in 1Cr-0.5Mo steel can be summarised as shown in Table 1.

Table 1:

Evolution of creep cavities in 1Cr-0.5Mo steel

Creep cavity	Average initial cavity radius R_i (μm)	Average cavity radius $R_c(\mu m)$ at coalescence stage	Percentage change in cavity radius $\left\|\frac{R_i - R_r}{R_r}\right\|$
Semi-minor axis	0.433	0.430	0.7%
Semi-major axis	0.778	0.956	18.6%
Observation	The coalescence of cavities to form micro-cracks appeared at rupture time. A slight decrease of cavity radius in the semi-minor axis direction was observed. An increase of cavity radius in the semi-major axis direction was observed. Within areas of the same size, initial cavity density was approximately 10 times less than the cavity density at coalescence stage. Cavities associated with particles were observed at coalescence stage.		

Table 1 summarises the evolution of creep cavity in 1Cr-0.5Mo steel. The percentage change in cavity radius was not obvious in the semi-minor axis direction, but the percentage change in cavity radius in the semi-major axis direction increased by approximately 20% from the initial damage stage to coalescence stage. The cavities on the GB were constrained by the GB and surrounding material [22], as the growth of the cavities' radii in the semi-minor

axis direction were restricted by the width of the GB. Furthermore, the size of newly nucleated cavities was not large as a result of a slight decrease in the average cavity radius in the semi-minor axis direction. The number of cavities increased significantly from initial damage stage to coalescence stage because this experiment was conducted under low stress level, and thus the dominative rupture mechanism was based on cavity nucleation. However, an increase in cavity radius in the semi-major axis direction was observed. Such behaviour may have been caused by the occurrence of high local stresses during the damage process and the fact that the rupture mechanism based on cavity growth promotes the growth of cavity radii in the semi-major axis, which is along the transverse GB direction. Thus, the creep rupture process in 1Cr-0.5Mo steel is not only dependent on cavity nucleation but also affected by cavity growth. Although the observation was conducted at a low stress level, high local stresses caused by the stress breakdown phenomenon can also change the dominative rupture mechanism in specific areas where such high local stress occurs.

4. Design the creep rupture criterion and damage equation

Cavities are often initiated at the intersection of a slip band with a GB or at ledges in the boundaries [23, 24]. The cavitated area fraction changes when the stress level changes. Furthermore, strain at failure increases in a nonlinear manner with the increase of stress level, as the damage varies with the stress level. With experiment data for the evolution of creep cavity for 2.25Cr-1Mo steel under stresses of 55.6MPa, 60.6MPa and 70.6MPa at a temperature of 565℃, the relationship between area fraction of cavitation and rupture time can be plotted as shown in Fig.5.

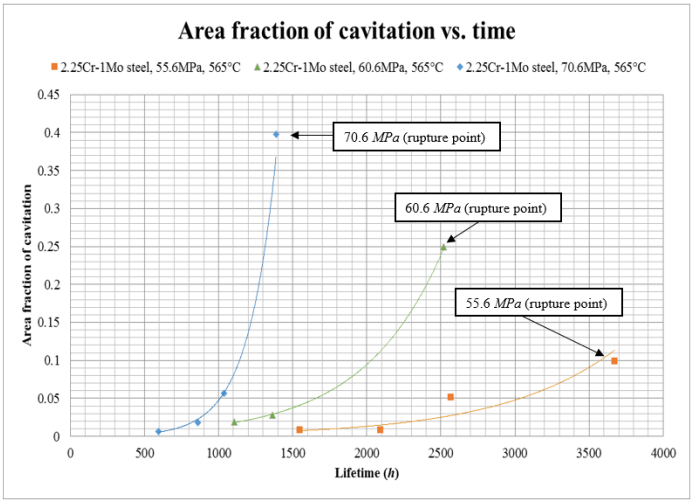

Fig.5: Area fraction of cavitation versus time for 2.25Cr-1Mo under the stresses 55.6MPa, 60.6MPa and 70.6MPa at temperature of 565℃

Fig.5 shows that the area fraction of cavitation increases in a nonlinear manner with time. Based on the limited experiment data available (only a small volume) describing the evaluation of creep cavity under different stresses for low Cr alloys, the relationship between area fraction of cavitation and stresses can be simply plotted as shown in Fig.6.

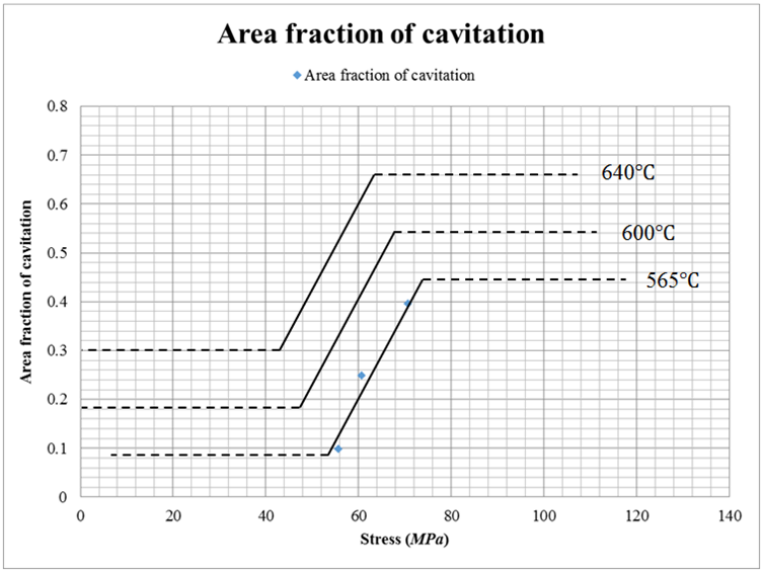

Fig.6: Area fraction of cavitation at rupture time versus stress for 2.25Cr-1Mo under the stresses 55.6MPa, 60.6MPa and 70.6MPa at temperature of 565℃, and assumption of the area fraction of cavitation at 600℃ and 640℃

The use of a fixed value as a rupture criterion has obvious limitations. Dyson and Osgerby [9] suggested that the percentage of boundary area fraction may be a suitable creep rupture criterion. They reported that in a uniaxial creep test, the failure condition was met when all of the grain boundaries normal to the applied load were completely cavitated. The area fraction of such cavities at failure is approximately 1/3, and since the damage variable represents a cavitated area fraction, then the damage at failure is equal to 1/3. The main advantage of using the percentage of boundary area fraction method is that cavity size and shape can be detected at the fracture surface in a physically-based experimental creep test.

Fig.6 shows the area fraction of cavitation at rupture time versus stress for 2.25Cr-1Mo under the stresses 55.6MPa, 60.6MPa and 70.6MPa at a temperature of 565℃, and an assumption of the area fraction of cavitation at 600℃ and 640℃. According to Fig.6, the area fraction of cavitation at rupture time obviously differs under the different stress levels and is not a fixed value. Thus, the use of a fixed value as rupture criterion has obvious limitations.

The area fraction at rupture time in Fig. 5 increases with the increase of stress level, and an approximately linear increase occurs at an intermediate stress level ($0.4\sigma_Y$-$0.5\sigma_Y$). Thus, the new damage creep rupture criterion can be described as follows:

$$\omega_c = \begin{cases} a & 0.2\sigma_Y \le \sigma \le 0.4\sigma_Y \\ \alpha\sigma - \delta & 0.4\sigma_Y \le \sigma \le 0.5\sigma_Y \\ b & \sigma > 0.5\sigma_Y \end{cases} \quad (5)$$

Where α and δ are the material parameters and σ is the applied stress. It should be noted that at relatively low stress level ($0.2\sigma_Y$-$0.4\sigma_Y$) and high stress level ($>0.5\sigma_Y$), the rupture criterion is shown as an approximately constant value in Fig.8. Moreover, the cavity density is affected by temperature. The degree of cavity nucleation and growth increases with the increase of temperature; therefore, in the absence of any other relationship between relative creep cavitation rupture area and stress, further assumptions can be made as plotted in Fig.8.

The proposed damage evolution equation has been extended to include stress dependence using Dyson's damage model. According to [9, 10], the creep damage variables D_N and $D_G$are proposed to describe the cavity nucleation damage mechanism and cavity growth damage mechanism respectively. The dimensionless damage parameter D_N demonstrates the area fraction of GB facets cavitated. When cavity evolution is growth controlled, the rate of cavity nucleation is $\dot{D}_N = 0$. When cavities are nucleated continuously, the evolution of D_N can be written as:

$$\dot{D}_N = N\left(\frac{K_N}{\varepsilon_{fu}}\right)\dot{\varepsilon} \quad (6)$$

The parameter of K_N has a maximum value of $1/3$, where ε_{fu} is the uniaxial strain at failure.

The dimensionless damage parameter D_G demonstrates the volume fraction of GB facets cavitated. When creep damage is cavity growth controlled, the rate of cavity growth can be written as:

$$\dot{D}_G = \frac{d}{2lD_G}\dot{\varepsilon} \quad (7)$$

Where l is the inter-cavity spacing and d is the grain size [24]

By coupling with the cavity nucleation damage mechanism and cavity growth damage mechanism, Dyson's damage evolution equation can be written as:

$$\dot{\omega} = C\dot{\varepsilon} \quad (8)$$

Where C is the material parameter; $\dot{\varepsilon}$ is the creep strain rate and $\dot{\omega}$ is the damage rate. The use of creep damage variables D_N and D_G can be decided by the parameter C [10].

However, the creep rupture process in low Cr alloy steel is not only dependent on cavity nucleation but also affected by cavity growth at the same time. At low stress levels, due to the creep rupture mechanism, it is suggested that the evolution of cavity is the result of continuous cavitation nucleation and a constrained cavity growth mechanism, which has a dominant influence on the accumulation of damage leading to final rupture behaviour.

According to Table 1, the occurrence of high local stresses during the damage process and the fact that the rupture mechanism based on cavity growth promotes the growth of cavity radii in the semi-major axis, which is along the transverse GB direction. Although the observation was conducted at a low stress level, high local stresses caused by the stress breakdown phenomenon can also change the dominative rupture mechanism in specific areas where such high local stress occurs. Thus, a strain exponent should be implemented into Dyson's respected damage model and the improved damage evolution equation can be written as:

$$\dot{\omega} = C\dot{\varepsilon}^{x} \tag{9}$$

Where C and x are the material parameter and strain exponent, respectively; $\dot{\varepsilon}$ is the creep strain rate and $\dot{\omega}$ is the damage rate.

5. Validation of the creep ruptures criterion and damage equation

Experiment data for the evolution of creep damage under the stress 40MPa ($0.31\sigma_Y$) at 640℃ for 0.5Cr0.5Mo0.25V base material are utilized to demonstrate the validity of the creep rupture criterion. Furthermore, Dyson's conventional criterion was investigated, and the simulated results compared with experiment data and the result from the newly developed damage evolution equation.

With the stress 40MPa and the time increment of 50 hours, comparison of the newly developed damage evolution equation with the experiment data for 0.5Cr0.5Mo0.25V base material can be plotted as shown in Fig.7.

Fig.7 shows the comparison of the newly developed damage evolution equation with the experiment data for 0.5Cr0.5Mo0.25V base material. The creep strain predicted by the newly developed damage evolution equation is in good agreement with the experiment data from the initial time to rupture time.

In order to clearly compare the creep strain predicted by the newly developed damage evolution equation and Dyson's damage evolution equation, simulated results from the two different models are plotted in Fig.8.

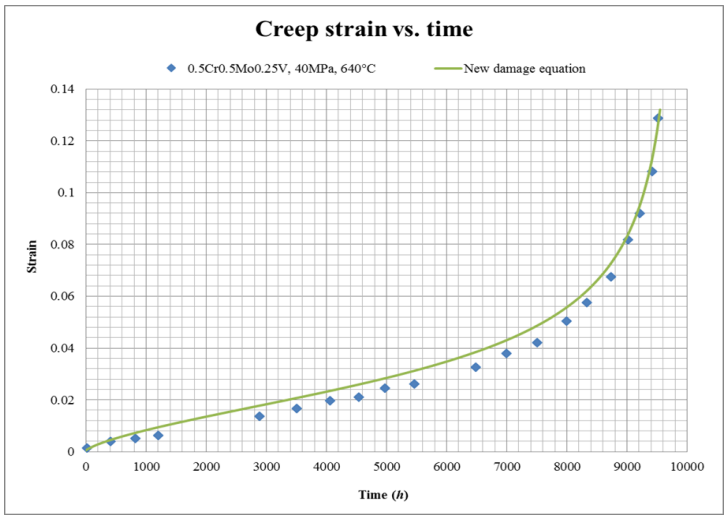

Fig.7: Comparison of newly developed damage evolution equation with the experiment data for 0.5Cr0.5Mo0.25V base material

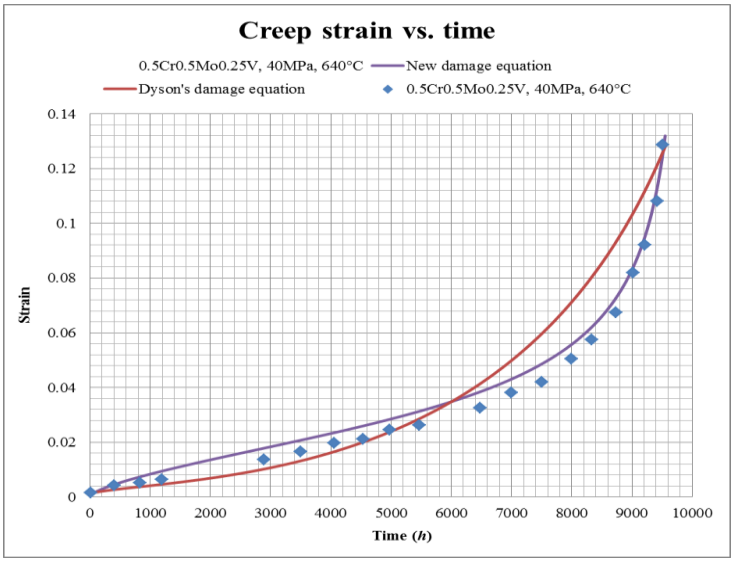

Fig.8: Comparison of newly developed damage evolution equation with Dyson's damage evolution equation for 0.5Cr0.5Mo0.25V base material

Fig.8 shows the comparison of the newly developed damage evolution equation with Dyson's damage evolution equation for 0.5Cr0.5Mo0.25V base material. According to Fig.11, the creep strain predicted by the newly developed damage evolution equation fits much better with the experiment data than that predicted by Dyson's damage evolution equation.

6. Conclusions

This paper firstly reports the evolution of creep cavity during the rupture process, and the creep mechanisms involved in the rupture process of low Cr alloys under long-term service have been determined. Secondly, a new rupture criterion for constitutive equations has been proposed. It also illustrates why the typical rupture criteria do not satisfy the requirements for developing creep damage constitutive equations. Thirdly, a new damage evolution equation has been proposed, and validation of the damage evolution equation has been presented which shows the results to be in good agreement with those of the experiment test. This work contributes to computational creep damage mechanics in general and particularly to the design and development of a constitutive model for creep damage analysis of low Cr alloys under long-term service.

Acknowledgments

This paper is supported by Youth Project of Hubei Provincial Department of Education (No.Q20172603). The author gratefully acknowledges the technologies support of Dr. Qihua Xu and Wuhan National Laboratory for Optoelectronics, Huazhong Institute of Electro-Optics.

R E F E R E N C E S

[1]. *A. Zieliński, G. Golański and M. Sroka*, Comparing the methods in determining residual life on the basis of creep tests of low-alloy Cr-Mo-V cast steels operated beyond the design service life, International Journal of Pressure Vessels and Piping, **Vol.** 152 (2017), P. 1-6.

[2]. *Q.H. Xu, Q. Xu, Y.X. Pan and M. Short*, Review of creep cavitation and rupture of low Cr alloy and its weldment, Advanced Materials Research, **Vol.** 744(744) (2013), P. 407-411.

[3]. *G. Zhang, C. Zhou, Z. Wang, F. Xue, Y. Zhao and L. Zhang*, Numerical simulation of creep damage for low alloy steel welded joint considering as-welding residual stress. Nuclear Engineering & Design, **Vol.** 242 (2012), P. 26-33.

[4]. *Y.S. Garud*, Low temperature creep and irradiation creep in nuclear reactor applications: a critical review, International Journal of Pressure Vessels and Piping, **Vol.** 139–140 (2016), P. 137-145.

[5]. *A. Bozorg-Haddad and M. Iskander*, Predicting compressive creep behavior of virgin hdpe using thermal acceleration, Journal of Materials in Civil Engineering, **Vol.** 23(8) (2011), P. 1154-1162.

[6]. *B.M. Morrow, R.W. Kozar, K.R. Anderson and M.J. Mills,* An examination of the use of the modified jogged-screw model for predicting creep behavior in zircaloy-4, Acta Materialia, **Vol.** 61(12) (2013), P. 4452-4460.

[7]. *D.Z. Liu, Q. Xu, Z.Y. Lu, D.L. Xu and Q.H. Xu,* The techniques in developing finite element software for creep damage analysis Advanced Materials Research, **Vol.** 744 (2013), P. 199-204.

[8]. *J. Christopher and B.K. Choudhary*, Sine hyperbolic models and their applicability towards creep deformation behaviour of 9% chromium steels, Transactions of the Indian Institute of Metals, **Vol.** 70(3) (2017), P.1-6.

[9]. *B.F. Dyson and S. Osgerby*, Mathematical modelling of creep/environment interactions, Sadhana, **Vol.** 20(1) (1995), P.185-198.
[10]. *B.F. Dyson*, The ridged uniaxial test piece: creep and fracture predictions using large-displacement finite-element analyses, Proceedings of the Royal Society A, **Vol.** 452(1946) (1996), P. 655-676.
[11]. *S. Goyal, K. Laha, C.R. Das and M.D. Mathew*, Analysis of creep rupture behavior of Cr-Mo ferritic steels in the presence of notch, Metallurgical & Materials Transactions A, **Vol.** 46(1) (2015), P. 205-217.
[12]. *X. Xu, G.Z. Wang, F.Z. Xuan and S.T. Tu*, Effects of creep ductility and notch constraint on creep fracture behavior in notched bar specimens, Materials at High Temperatures, **Vol.** 33(2) (2016), P. 1-10.
[13]. *Q.H. Xu, Q. Xu, Y.X. Pan and M. Short*, Current state of developing creep damage constitutive equation for 0.5Cr0.5Mo0.25V ferritic steel, Advanced Materials Research, **Vol.** 510(2) (2012), P. 812-816.
[14]. *Q.H. Xu, Q. Xu, Z.Y. Lu and S. Barrans*, A review of creep deformation and rupture mechanisms of cr-mo alloy for the development of creep damage constitutive equations under lower stress, Journal of Communication and Computer, **Vol.** 10(9) (2013), P. 1219-1228.
[15]. *Y. Kadoya and T. Goto*, Creep deformation and creep-rupture behaviour of Cr-Mo-V steel forgings, Isij International, **Vol.** 30(10) (2009), P. 829-837.
[16]. *T. Sakthivel, S.P. Selvi, P. Parameswaran and K. Laha*, Creep deformation and rupture behaviour of thermal aged p92 steel, submitted to Materials at High Temperatures, **Vol.** 33 (1) (2016), P. 33-43.
[17]. *A.I. Petrov and M.V. Razuvaeva*, Effect of pressure on the lifetime and the creep of metals and the kinetic equation parameters, Technical Physics, **Vol.** 60(9) (2015), P. 1326-1329.
[18]. *T.R. Stepanova and T.V. Prokhorova*, Modeling of the high temperature creep and rupture under the complex stress state, Materials Science Forum, **Vol.** 870 (2016), P. 528-534.
[19]. *D.R. Hayhurst, J. Lin and R.J. Hayhurst*, Failure in notched tension bars due to high-temperature creep: interaction between nucleation controlled cavity growth and continuum cavity growth, International Journal of Solids & Structures, **Vol.** 45(7) (2008), P. 2233-2250.
[20]. *E.V.D. Giessen and V. Tvergaard*, A creep rupture model accounting for cavitation at sliding grain boundaries, International Journal of Fracture, **Vol.** 48(3) (1991), P. 153-178.
[21]. *J. Dobrzański,* Computer assisted classification of internal damages in the 10CrMo9-10 steel working in creep service [J], International Journal of Computational Materials Science & Surface Engineering, **Vol.** 1(6) (2007), P. 706-716.
[22]. *J. He and R. Sandström*, Creep cavity growth models for austenitic stainless steels, Materials Science & Engineering A, **Vol.** 674 (2016), P. 328-334.
[23]. *J.O. Chung, J. Yu and S.H. Hong*, Steady-state creep crack growth by continually nucleating cavities, Journal of the Mechanics & Physics of Solids, **Vol.** 38(1) (1990), P. 37-53.
[24]. *M. Sauzay and M.O. Moussa*, Prediction of grain boundary stress fields and microcrack initiation induced by slip band impingement, International Journal of Fracture, **Vol.** 184(1-2) (2013), P. 215-240.